JOURNAL OF GEOPHYSICAL RESEARCH, VOL. 112, A06217, doi:10.1029/2006JA012174, 2007

The plasmapause response to the southward turning of the IMF derived from sequential EUV images

Go Murakami,[1] Mariko Hirai,[1] and Ichiro Yoshikawa[1]

Received 14 November 2006; revised 20 January 2007; accepted 29 January 2007; published 13 June 2007.

[1] We statistically examined the plasmapause response to the southward turning of the interplanetary magnetic field (IMF) using sequential global images of the plasmasphere, in order to understand how the convection electric field propagates to the inner magnetosphere. The extreme ultraviolet (EUV) imager on the Imager for Magnetopause-to-Aurora Global Exploration satellite clearly observed inward motion of the plasmapause driven by the southward turning of the IMF. We surveyed the EUV data in the 2000–2001 period and found 16 events. Using the sequential EUV images, we calculated the plasmapause radial velocity, and then estimated the time development of the convection electric field at the plasmapause (E_{pp}). E_{pp} and the solar wind electric field derived from the measurement by the ACE satellite had very similar variations each other, but there surely was a time lag. Consequently, our research indicates that the plasmapause response to the southward turning of the IMF takes 10–30 min. This timescale suggests that the convection electric field penetrates from the magnetopause to the inner magnetosphere through the ionosphere.

Citation: Murakami, G., M. Hirai, and I. Yoshikawa (2007), The plasmapause response to the southward turning of the IMF derived from sequential EUV images, *J. Geophys. Res.*, *112*, A06217, doi:10.1029/2006JA012174.

1. Introduction

[2] The plasmapause is the outer boundary of the Earth's plasmasphere which is a torus-shaped region filled with cold plasmas in the inner magnetosphere. Decades of observation show that the radial location of the plasmapause generally moves inward during geomagnetic disturbance periods. The inward motion is explained by a longstanding hypothesis that the dynamics of the plasmasphere is controlled by the superposition of the corotation and convection electric field [*Nishida*, 1966]. The enhanced convection electric field triggered by the southward turning of the IMF forms new $E \times B$ drift trajectories, and plasmas on the plasmapause move inward along them [*Chappell et al.*, 1970].

[3] Some other mechanisms explaining the inward motion of the plasmapause during geomagnetic disturbance periods have been proposed. *Lemaire* [1974, 1985] proposed that the centrifugal force drives the plasma upwards and then produces a sharp density gradient along the magnetic field lines tangent to the zero parallel force (ZPF) surface. According to this mechanism, after an increase in the level of magnetic activity the ZPF surface shifts inward and the plasmasphere is peeled off in the post midnight sector where the convection velocity is maximum [*Lemaire and Gringauz*, 1998]. *Carpenter and Lemaire* [1997] discussed the loss of plasmas through the flow from the plasmasphere into the underlying ionosphere during periods of the enhanced convection. They indicated the possibility of the mechanism involving dumping of plasmas into the ionosphere based on the whistler data.

[4] Although it is not completely understood how the convection electric field governing the dynamics mentioned above propagates to the inner magnetosphere, a number of observational studies have examined the ionospheric response to the IMF. For example, the ionospheric convection responds to the IMF quickly (~10 min) [*Ridley et al.*, 1998] and almost simultaneously at the whole ionosphere [*Kikuchi et al.*, 1996; *Ruohoniemi and Greenwald*, 1998; *Ridley et al.*, 1998; *Lu et al.*, 2002]. Furthermore, using the ground magnetometers, *Hashimoto et al.* [2002] examined the response time of the convection in the inner magnetosphere to the enhancement of the ionospheric convection. Their study suggests that the convection electric field propagates from the dayside magnetopause to the nightside inner magnetosphere through the ionosphere.

[5] With regard to experimental work on the plasmasphere, the conventional extreme ultraviolet (EUV) photometric experiments from an inside-out view, which had been done intensively in the 1970s, suggested that the Earth's plasmasphere would be imaged by He II (30.4 nm) emission [e.g., *Johnson et al.*, 1971]. In the 1990s, the remote-sensing method using the EUV emission became a powerful tool to provide global perspectives on the plasmasphere dynamics [*Williams et al.*, 1992]. The fundamental technology to detect the EUV emission began with the He II emission through a rocket experiment [*Yoshikawa et al.*, 1997]. The two-dimensional He II imaging of the terrestrial plasmasphere from its outside was first done by the

[1]Department of Earth and Planetary Science, Graduate School of Science, The University of Tokyo, Tokyo, Japan.

0148-0227/07/2006JA012174$09.00

Planet-B (Nozomi) spacecraft [*Nakamura et al.*, 2000]. *Yoshikawa et al.* [2000a, 2000b, 2001] first presented static EUV images of the plasmasphere and the inner magnetosphere.

[6] Recent advances in satellite-based imaging techniques have made it possible to routinely obtain full global images of the plasmasphere. The EUV instrument on the Imager for Magnetopause-to-Aurora Global Exploration (IMAGE) satellite gave us complete sequential pictures (one image/10 min) [*Burch et al.*, 2001a, 2001b; *Sandel et al.*, 2000, 2001]. Using these sequential images, *Goldstein et al.* [2003b, 2003c, 2004a, 2005] and *Spasojević et al.* [2003] identified the correlation between the inward motion of the plasmapause and the southward turning of the IMF for specific events. They found that the timescale of the plasmapause response to the IMF is about 30 min in their case studies. Furthermore, *Pierrard and Cabrera* [2005, 2006] presented the simulations of the plasmapause formation and compared the predicted plasmapause positions with the EUV observations. They remarked the correlation between the inward motion of the plasmapause and the southward turning of the IMF in numerical simulations. However, they did not discuss the timescale of the plasmapause response to the IMF in their studies.

[7] In this study, we statistically examine the plasmapause response to the southward turning of the IMF in order to understand the propagation mechanism of the convection electric field in the inner magnetosphere. We survey the EUV data set in the period of May 2000–December 2001 obtained by the IMAGE satellite (available at http://euv.lpl.arizona.edu/euv/), and find the events showing the clear inward motion of the nightside plasmapause. Finally, we deduce the timescale of the plasmapause response to the southward turning of the IMF.

2. Data Selection

[8] The EUV instrument on the IMAGE satellite imaged the He^+ distribution in the plasmasphere by detecting resonantly scattered solar 30.4-nm radiation. The measured brightness is directly proportional to the He^+ column density along the line of sight because the 30.4-nm emission from the plasmasphere is optically thin [*Sandel et al.*, 2001]. The EUV imager consisted of three cameras, and their fields of view were overlapped to create a single image. It produced sequential images of the plasmasphere every 10 min for generally 7–9 hours out of each 14-hour orbit, with spatial resolution of $\sim$0.1 R_E as seen from the apogee ($\sim$8 R_E).

[9] Figure 1a shows two snapshots of the He^+ plasmasphere, taken at 02:29 and 04:32 UT on 22 April 2001 by the EUV imager. The black circle indicates the Earth and the white arrow points sunward in each image. The shadow of the Earth is seen in the antisunward direction, and the bright arc at the Earth's dayside limb is airglow from He and O^+ [*Burch et al.*, 2001a, 2001b]. The left side data are not available because throughout the event the camera whose field of view covered the duskside was usually turned off to prevent sunlight from entering the camera [*Goldstein et al.*, 2005]. The white squares indicate the manually identified plasmapause along the sharp brightness gradient.

[10] On the assumption that the plasmapause is field-aligned in the dipole magnetic field, the field line with the minimum L (radial distance in the equatorial plane) along the line of sight to each identified point is found. Then we can map the plasmapause to the magnetic equatorial plane along the field line, like *Goldstein et al.* [2003a]. There is some subjectivity involved in manually extracting the plasmapause. We repeated this manual extraction of the plasmapause and calculated the dispersion of the identified plasmapause locations. As a result, we estimated that the uncertainty due to the subjectivity was about 0.2 R_E, which is consistent with that reported in *Goldstein et al.* [2003a, 2005]. Figure 1b shows the plasmapause locations at 02:29 and 04:32 UT on 22 April 2001 mapped to the magnetic equatorial plane using this method. It is clear that the nightside plasmapause at 04:32 UT is about 1.5 R_E closer to the Earth than that at 02:29 UT in Figure 1b.

[11] To investigate the inward motion of the plasmapause driven by the southward turning of the IMF, we searched the EUV data set in the period of May 2000-December 2001, and identified 16 events according to the following criteria:

[12] –The northward IMF continued more than 10 min before the southward turning.

[13] –The IMF turned southward more rapidly than 0.25 nT/min.

[14] –The southward IMF continued more than 10 min after the turning.

[15] –The EUV instrument clearly observed the sharp plasmapause on the nightside and the whole inward motion of the nightside plasmapause in the field of view.

[16] Figure 2 shows an example of the variation of the IMF B_Z component (B_{IMF_Z}) satisfying the above criteria, measured by the MAG instrument onboard the ACE satellite [*Smith et al.*, 1998] on 22 April 2001. The IMF turned southward at 01:27 and 02:15 UT distinctly. We used 1-min interval data set of the IMF. We estimated the arrival time of every IMF at the average magnetopause (10 R_E) from the ACE position as follows.

[17] (1) We assumed that the every IMF measured by the MAG instrument continued to propagate and arrived at the magnetopause and that the magnitude and polarity of the IMF did not change.

[18] (2) We used the solar wind velocity data simultaneously measured by the SWEPAM instrument on the ACE satellite [*McComas et al.*, 1998] and assumed the velocity did not change. We calculated the arrival time of every IMF at the magnetopause based on the position of the ACE satellite.

[19] (3) We labeled every IMF the arrival time at the magnetopause. This method provides more correct information than by simply assuming a constant velocity of the solar wind.

3. Analysis

[20] In Figure 1a, the sharp He^+ edge is identified in the EUV image, and it corresponds to the plasmapause [*Roelof and Skinner*, 2000; *Goldstein et al.*, 2003a]. We mapped the plasmapause in the EUV images to the equatorial plane, as shown in Figure 1b. Using centered time differencing of the sequential plasmapause positions, we calculated the plasma-

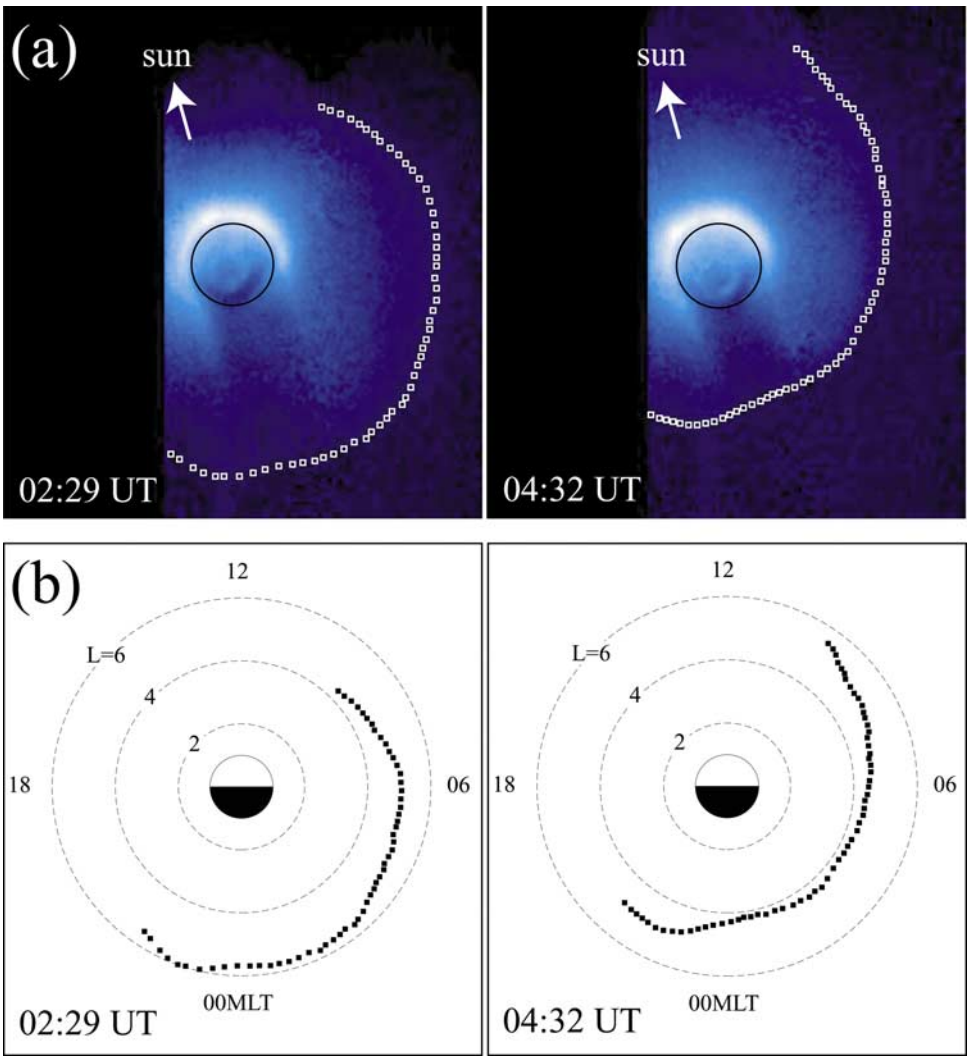

Figure 1. (a) Images of the He^+ plasmasphere taken by the EUV instrument on 22 April 2001. The black circle indicates the Earth and the white squares indicate the manually identified plasmapause in the EUV images. The left side data are not available. (b) The plasmapause of each image mapped to the magnetic equatorial plane. The black squares indicate the manually identified plasmapause in the magnetic equatorial plane, and the dashed circles are drawn at $L = 2, 4, 6$. The nightside plasmapause at 04:32 UT is about 1.5 R_E closer to the Earth than that at 02:29 UT.

pause radial velocity (V_{pp}) at the particular MLT where the plasmapause was clearly identified and the inward motion was most pronounced. For example, Figure 3 shows the variation of V_{pp} at 2.1 MLT on 22 April 2001. V_{pp} has the subjective error due to the subjectivity in manually extraction of the plasmapause (0.2 R_E) as mentioned in the previous section. Using this value, we estimated that the average uncertainty in V_{pp} was about ±0.4 R_E/hour, which is consistent with that discussed by *Goldstein et al.* [2003a, 2003b]. As seen in Figures 2 and 3, B_{IMF_Z} and V_{pp} have very similar variations with a time lag.

[21] The solar wind and IMF impose an electric field potential across the magnetosphere, driving the convection. Therefore to examine the correlation between the plasmapause motion and the IMF turning, it is meaningful to express both in electric field parameters. Figure 4 shows a schematic diagram of the inward plasmapause motion in the enhanced electric field. On the assumption that the plasmas on the plasmapause move by $E \times B$ drift as described in Figure 4, we represent the plasmapause motion as the electric field parameter (E_{pp}) defined as

$$E_{pp} \equiv -V_{pp} \times B_{dipole}, \quad (1)$$

where B_{dipole} is the equatorial dipole geomagnetic field. We calculate B_{dipole} using a simple dipole formula, $B_{dipole} = B_E/L^3$ ($B_E = 3.11 \times 10^{-5}$ T). E_{pp} approximately corresponds to the convection electric field in the midnight region. The variation of E_{pp} is dominated by that of V_{pp} because B_{dipole} is smooth. Similarly, we represent the variation of the IMF as the electric field of the solar wind (E_{sw}) defined as

$$E_{sw} \equiv -V_{sw} \times B_{IMF\_Z}, \quad (2)$$

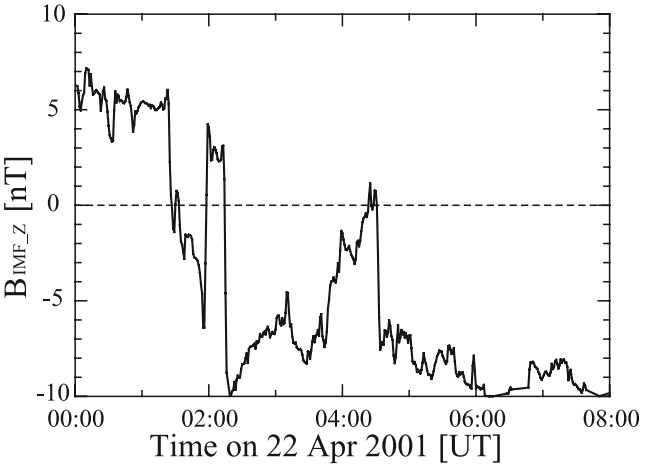

Figure 2. The 1-min interval data set of the IMF B_z component (in GSM coordinates) on 22 April 2001 measured by the MAG instrument onboard the ACE satellite. We have compensated the arrival time of every IMF at the average magnetopause (10 R_E) from the ACE position (~213 R_E), taking into account the variation of the solar wind velocity.

where V_{sw} is the solar wind velocity. We used V_{sw} data measured by the SWEPAM instrument onboard the ACE satellite.

[22] Then we calculated the linear correlation coefficient between E_{pp} and E_{sw} with various time delays, to investigate the response time of the plasmapause to the IMF. Figure 5 shows the correlation coefficient on 22 April 2001. The maximum value of the correlation is 0.73 when we assume a 16-min delay. Because of the interval of the EUV data set

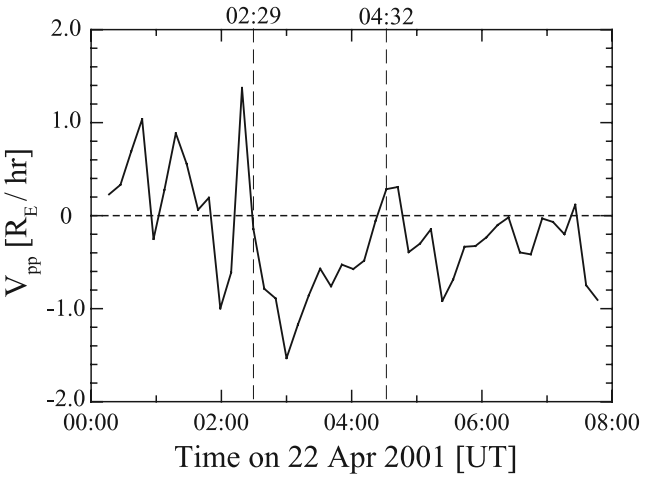

Figure 3. Radial plasmapause velocity (V_{pp}) on 22 April 2001 at 2.1 MLT where the inward motion of the nightside plasmapause was most pronounced. $V_{pp} < 0$ indicates that the plasmapause moves inward. The prominent inward motion of the plasmapause occurs in the period between 02:29 and 04:32 UT, and the locations of the plasmapause at both times are presented in Figure 1. The error of V_{pp} due to the manually extraction of the plasmapause is about ±0.4 R_E/hour.

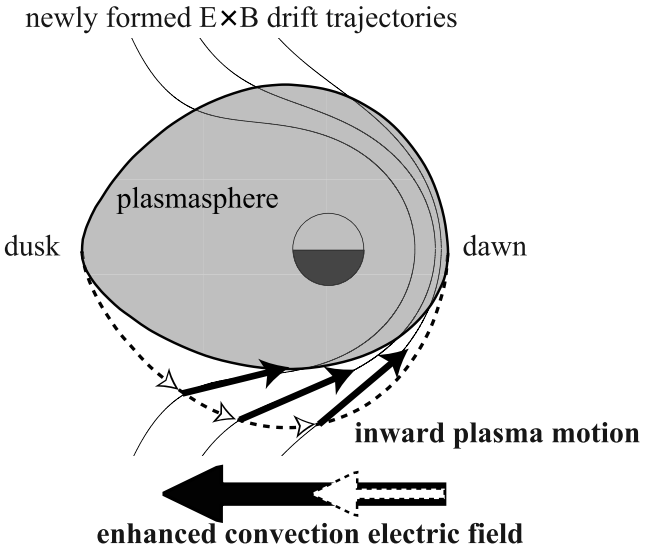

Figure 4. A schematic diagram of the inward plasma motion at the nightside plasmapause, in the convection electric field enhanced by the southward turning of the IMF. The dashed line indicates the previously formed plasmapause at the nightside. After the enhancement, the plasmas on the previous plasmapause move inward as black arrows along the newly formed $E \times B$ drift trajectories.

(10 min) and the subjective error in V_{pp}, the response time calculated in our method has some uncertainty. For reference, therefore, the range of 90% of the maximum correlation value is displayed in Figure 5. Both E_{pp} and 16-min delayed E_{sw} are shown in Figure 6, where E_{pp} multiplied by 5 is displayed to show both quantities in the same magnitude. The number of 5 suggests that the solar wind electric field penetrates in the inner magnetosphere by 20%. This is consistent with the result of 10–25% reported in previous studies [*Goldstein et al.*, 2003b, 2003c, 2004b, 2005]. As seen in Figure 6, E_{pp} and E_{sw} are clearly correlated.

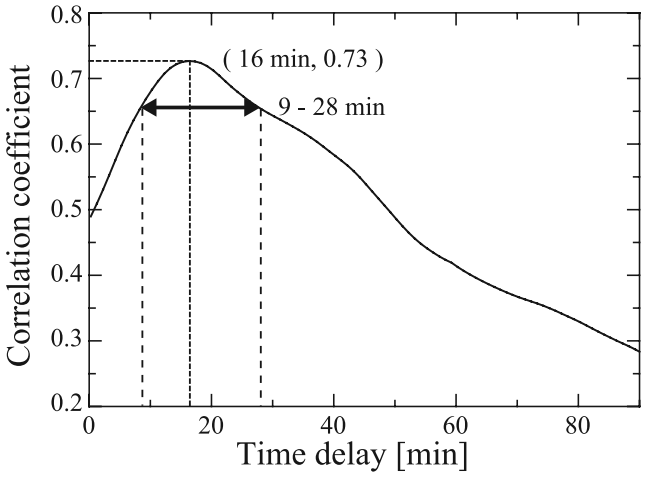

Figure 5. The correlation coefficient between the electric field parameters at the plasmapause (E_{pp}) and in the solar wind (E_{sw}) on 22 April 2001. The maximum value of the correlation is 0.73 at a 16-min delay. The range of 90% of the maximum correlation value is also displayed.

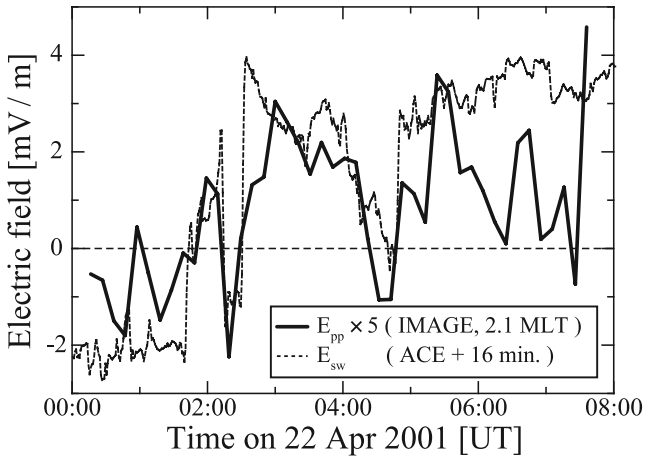

Figure 6. Electric field parameters E_{pp} (plasmapause) and E_{sw} (solar wind). The variations of E_{pp} and E_{sw} are qualitatively the same as V_{pp} and B_{IMF_Z}, respectively. E_{sw} is displayed with 16-min delay, which is the best correlated time delay between E_{pp} and E_{sw}. E_{pp} has been multiplied by 5 in order to show both quantities in the same magnitude.

[23] For the other events, we calculated the correlation coefficient in the same way. Table 1 and Figure 7 show the results. We regard the best-correlated time delay between E_{pp} and E_{sw} as the timescale of the plasmapause response to the IMF variation. There are four events in which the maximum values of the correlation coefficient are below 0.5 in Table 1. Among four events, there is common aspect that the IMF has a shortly periodical structure and therefore there are several local maximum values in the correlation coefficient. That decreases the overall maximum value in the correlation coefficient. Nevertheless, these events also imply that the plasmapause responded to the southward turning of the IMF. We include these four events in our results. Finally, our results indicate that the plasmapause response to the southward turning of the IMF takes 10–30 min, and average 18 min.

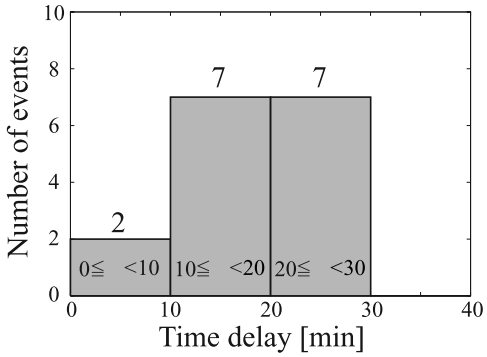

Figure 7. The histogram of the time delay between E_{pp} and E_{sw} listed in Table 1. It corresponds to the response time of the plasmapause to the IMF variation.

4. Discussion

[24] The timescale of the plasmapause response to the southward turning of the IMF derived from the sequential EUV images was studied for specific events. Table 1 shows the results of the previously published case studies. For example, *Goldstein et al.* [2003b] found that the response time on 10 July 2000 is 30 min at 2.4 MLT, while it is

Table 1. The Event List Showing the Date, MLT Where we Calculated the Radial Plasmapause Velocity, the Maximum Value of the Correlation Coefficient Between E_{pp} and E_{sw}, the Best Correlated Time Delay, Time Delay Variation Among 90% of the Maximum Correlation Value, the Solar Wind (SW) Propagation Time From the ACE Satellite to the Magnetopause in our Study, and Previously Published Studies

	This study					Previous case study	
Date	MLT	Correlation	Delay (min)	90% range (min)	SW propagation (min)	Delay (min)	SW propagation (min)
29 May 2000	4.0	0.79	21	16–27	61		
2 Jun 2000	0.0	0.67	23	18–28	54		
3 Jun 2000	0.2	0.46	0	0–20	57		
8 Jun 2000	3.0	0.47	22	17–27	44		
10 Jul 2000	2.0	0.68	28	13–41	60	30[a]	63[b]
28 Jul 2000	0.4	0.51	23	19–28	56		
5 Aug 2000	0.0	0.49	19	13–26	51		
17 Aug 2000	2.0	0.54	19	7–33	62		
28 Aug 2000	1.5	0.58	13	7–21	43		
6 Feb 2001	1.6	0.66	10	3–34	70		
22 Apr 2001	2.1	0.73	16	9–28	60	27[c]	63
28 May 2001	2.8	0.51	18	0–38	46		
1 Jun 2001	3.0	0.59	0	0–26	71		
2 Jun 2001	1.0	0.59	24	18–32	58	32[d]	55
21 Jun 2001	3.0	0.58	15	6–27	43		
26 Jun 2001	3.0	0.45	29	24–50	52	32[e]	54.8

[a][*Goldstein et al.*, 2003b].
[b]*Goldstein et al.* [2003b] used the IMF data set measured by the Geotail satellite. They assumed the constant solar wind velocity of ~400 km/s and calculated the solar wind propagation time by 3.7 min based on the Geotail position (~24 R_E). We extrapolated the propagation time from the ACE position (~238 R_E).
[c][*Goldstein et al.*, 2005].
[d][*Goldstein et al.*, 2003c, 2004a].
[e][*Spasojević et al.*, 2003].

28 min at 2.1 MLT in our study. Also, *Spasojević et al.* [2003] reported that on 26 June 2001, the response time is 32 min, and by our method it is 29 min. The results of our research for these two events are consistent with those of their case studies. However, as shown in Table 1, the response times on 2 June 2001 and 22 April 2001 in our results are different from those reported by *Goldstein et al.* [2003c, 2004a] and *Goldstein et al.* [2005] by ~10 min. In spite of using almost the same techniques to determine the response time of the plasmasphere to the IMF as theirs, our estimates show shorter response times than those in their studies. These discrepancies would mainly result from the difference in the method to compensate the propagation time of the IMF from the satellite to the magnetopause. *Goldstein et al.* [2003c, 2004a, 2005] assumed the constant solar wind velocity. We also calculated the response time using their method and found the same result. But in order to calculate the correlation more precisely, we took into account the variation of the velocity.

[25] The plasmapause response to the southward turning of the IMF provides important information about the complex coupling of the inner/outer magnetosphere, ionosphere, and solar wind. When the southward IMF arrives at the dayside magnetopause, the convection electric field is first enhanced in the ionosphere, driven by the polar cap potential. Many observational studies have examined the ionospheric response to the IMF [e.g., *Hairston and Heelis*, 1995; *Ruohoniemi and Greenwald*, 1998; *Ridley et al.*, 1998; *Lu et al.*, 2002]. *Ridley et al.* [1998] investigated the electric potential in the ionosphere using the ground magnetometers, and found that the ionospheric convection starts to change with a time lag of 8.4–13.6 min from the arrival of the IMF at the magnetopause. In addition, the ionospheric convection occurs almost simultaneously (within 2 min) at all local times [*Ruohoniemi and Greenwald*, 1998; *Lu et al.*, 2002] and whole latitudes [*Kikuchi et al.*, 1996]. After the enhancement of the ionospheric convection, the enhanced convection electric field would propagate from the ionosphere to the inner magnetosphere along the magnetic field lines [*Hashimoto et al.*, 2002]. Using the ground magnetometers, *Hashimoto et al.* [2002] found that the response time of the convection in the inner magnetosphere to the enhancement of the ionospheric convection takes 5–11 min. Totally, from the observational studies of the ionospheric convection mentioned above, we estimate that the propagation time of the convection electric field from the dayside magnetopause to the nightside plasmapause is 13–25 min. This timescale is consistent with our result of 10–30 min.

[26] We need to discuss another possible propagation mechanism. For example, the penetration of the convection electric field from the magnetopause to the inner magnetosphere through the magnetotail is driven by the magnetic reconnection. After the dayside reconnection, the solar wind carries reconnected open field lines tailward. Then they reconnect again in the magnetotail and the earthward convection flow is enhanced. Finally, the enhanced convection electric field reaches the nightside inner magnetosphere.

[27] We estimate the timescale that the convection electric field takes to propagate to the inner magnetosphere through the mechanism mentioned above. (1) We calculate the propagation time from the dayside magnetopause to the reconnection point in the magnetotail, on the assumption of the average location of the dayside magnetopause (X_{GSM} = 10 R_E) and the reconnection point in the near-Earth magnetotail (X_{GSM} = −30 R_E) and of the typical solar wind velocity (V_x = −400 km/s). It will take ~11 min. (2) We assume that the velocity of the earthward flow from the reconnection point is V_x =50 km/s, which corresponds to the typical flow velocity in the plasma sheet reported in the statistical studies of satellite observations [*Huang and Frank*, 1986; *Baumjohann et al.*, 1988]. The propagation time from the reconnection point (X_{GSM} = −30 R_E) to the nightside inner magnetosphere (X_{GSM} = −5 R_E) is estimated by ~53 min. Totally, we estimate that the propagation time in this mechanism is ~64 min. Furthermore, *Nagai et al.* [2005] studied the magnetic reconnection in the near-Earth magnetotail using the Geotail satellite data and found that it starts 60 min after the southward turning of the IMF. Our estimate is consistent with the timescale reported in their study.

[28] In comparison between the two mechanisms, the former mechanism is preferable to our result. Therefore our study suggests that the convection electric field penetrates from the magnetopause to the inner magnetosphere through the ionosphere. But this is not an exclusive mechanism. Further study is necessary.

5. Summary

[29] Using the sequential images of the plasmasphere observed by the EUV instrument on the IMAGE satellite, we examined the plasmapause dynamics. We have shown that the plasmapause response to the southward turning of the IMF takes 10–30 min, and average 18 min. It is consistent with the timescale derived from the ionospheric observations. Therefore it indicates that the electric field penetrates from the magnetopause to the inner magnetosphere through the ionosphere. However, due to the limited EUV data, we found only 16 events in our search. Future observation of the plasmasphere by the SELENE satellite from the lunar orbit [*Yoshikawa et al.*, 1997] will give us not only much more sequential images with higher time resolution but also a deeper understanding of the plasmasphere dynamics from a different perspective.

[30] **Acknowledgments.** The authors would like to thank B. R Sandel for his assistance in the processing of EUV data available at http://euv.lpl.arizona.edu/euv/. We also thank N. Ness, C. Smith and the ACE science center for ACE MAG and D. McComas for ACE SWEPAM data.

[31] Wolfgang Baumjohann thanks Maria Spasojević and Fabien Darrouzet for their assistance in evaluating this paper.

References

Baumjohann, W., G. Paschmann, N. Sckopke, C. A. Cattell, and C. W. Carlson (1988), Average ion moments in the plasma sheet boundary layer, *J. Geophys. Res.*, *93*, 11,507.

Burch, J. L., et al. (2001a), Views of Earth's magnetosphere with the IMAGE satellite, *Science*, *291*(5504), 619.

Burch, J. L., D. G. Mitchell, B. R. Sandel, P. C. Brandt, and M. Wüest (2001b), Global dynamics of the plasmasphere and ring current during magnetic storms, *Geophys. Res. Lett.*, *28*(6), 1159.

Chappell, C. R., K. K. Harris, and G. W. Sharp (1970), A study of the influence of magnetic activity on the location of the plasmapause as measured by OGO 5, *J. Geophys. Res.*, *75*, 50.

Carpenter, D. L., and J. Lemaire (1997), Erosion and recovery of the plasmasphere in the plasmapause region, *Space Sci. Rev.*, *80*, 153.

Goldstein, J., M. Spasojević, P. H. Reiff, B. R. Sandel, W. T. Forrester, D. L. Gallagher, and B. W. Reinisch (2003a), Identifying the plasmapause in IMAGE EUV data using IMAGE RPI in situ steep density gradients, *J. Geophys. Res.*, *108*(A4), 1147, doi:10.1029/2002JA009475.

Goldstein, J., B. R. Sandel, W. T. Forrester, and P. H. Reiff (2003b), IMF-driven plasmasphere erosion of 10 July 2000, *Geophys. Res. Lett.*, *30*(3), 1146, doi:10.1029/2002GL016478.

Goldstein, J., B. R. Sandel, P. H. Reiff, and M. R. Hairston (2003c), Control of plasmaspheric dynamics by both convection and sub-auroral polarization stream, *Geophys. Res. Lett.*, *30*(24), 2243, doi:10.1029/2003GL018390.

Goldstein, J., B. R. Sandel, M. F. Thomsen, M. Spasojević, and P. H. Reiff (2004a), Simultaneous remote-sensing and in situ observations of plasmaspheric drainage plumes, *J. Geophys. Res.*, *109*, A03202, doi:10.1029/2003JA010281.

Goldstein, J., R. A. Wolf, B. R. Sandel, and P. H. Reiff (2004b), Electric fields deduced from plasmapause motion in IMAGE EUV images, *Geophys. Res. Lett.*, *31*(1), L01801, doi:10.1029/2003GL018797.

Goldstein, J., B. R. Sandel, W. T. Forrester, M. F. Thomsen, and M. R. Hairston (2005), Global plasmasphere evolution 22–23 April 2001, *J. Geophys. Res.*, *110*, A12218, doi:10.1029/2005JA011282.

Hairston, M. R., and R. A. Heelis (1995), Response time of the polar ionospheric convection pattern to changes in the north-south direction of the IMF, *Geophys. Res. Lett.*, *22*, 631.

Hashimoto, K. K., T. Kikuchi, and Y. Ebihara (2002), Response of the magnetospheric convection to sudden interplanetary magnetic field changes as deduced from the evolution of partial ring currents, *J. Geophys. Res.*, *107*(A11), 1337, doi:10.1029/2001JA009228.

Huang, C. Y., and L. A. Frank (1986), A statistical study of the central plasma sheet: Implications for substorm models, *Geophys. Res. Lett.*, *13*, 652.

Johnson, C. Y., J. M. Young, and J. C. Holmes (1971), Magnetoglow: A new geophysical resource, *Science*, *171*, 379.

Kikuchi, T., H. Lühr, T. Kitamura, O. Saka, and K. Schlegel (1996), Direct penetration of the polar electric field to the equator during a DP2 event as detected by the auroral and equatorial magnetometer chains and the EISCAT radar, *J. Geophys. Res.*, *101*, 17,161.

Lemaire, J. (1974), The 'Roche-limit' of ionospheric plasma and the formation of the plasmapause, *Planet. Space Sci.*, *22*, 757.

Lemaire, J. (1985), Frontiers of the Plasmasphere (Theoretical Aspects), Université Catholique de Louvain, Faculté des Sciences, Louvain-la-Neuve, ISBN 2-87077-310-2.

Lemaire, J. F., and K. I. Gringauz (1998), The Earth's plasmasphere, Cambridge Univ. Press, New York.

Lu, G., T. E. Holzer, D. Lummerzheim, J. M. Ruohoniemi, P. Stauning, O. Troshichev, P. T. Newell, M. Brittnacher, and G. Parks (2002), Ionospheric response to the interplanetary magnetic field southward turning: Fast onset and slow reconfiguration, *J. Geophys. Res.*, *107*(A8), 1153, doi:10.1029/2001JA000324.

McComas, D. J., S. J. Bame, P. Barker, W. C. Feldman, J. L. Phillips, P. Riley, and J. W. Griffee (1998), Solar Wind Electron Proton Alpha Monitor (SWEPAM) for the Advanced Composition Explorer, *Space Sci. Rev.*, *86*, 563.

Nagai, T., M. Fujimoto, R. Nakamura, W. Baumjohann, A. Ieda, I. Shinohara, S. Machida, Y. Saito, and T. Mukai (2005), Solar wind control of the radial distance of the magnetic reconnection site in the magnetotail, *J. Geophys. Res.*, *110*, A09208, doi:10.1029/2005JA011207.

Nakamura, M., I. Yoshikawa, A. Yamazaki, K. Shiomi, Y. Takizawa, M. Hirahara, K. Yamashita, Y. Saito, and W. Miyake (2000), Terrestrial plasmaspheric imaging by an extreme ultraviolet scanner on Planet-B, *Geophys. Res. Lett.*, *27*(2), 141.

Nishida, A. (1966), Formation of plasmapause, or magnetospheric plasma knee, by the combined action of magnetospheric convection and plasma escape from the tail, *J. Geophys. Res.*, *71*, 5669.

Pierrard, V., and J. Cabrera (2005), Comparisons between EUV/IMAGE observations and numerical simulations of the plasmapause formation, *Ann. Geophys.*, *23*, 2635.

Pierrard, V., and J. Cabrera (2006), Dynamical simulations of plasmapause deformations, *Space Sci. Rev.*, *122*, 119.

Ridley, A. J., G. Lu, C. R. Clauer, and V. O. Papitashvili (1998), A statistical study of the ionospheric convection response to changing interplanetary magnetic field conditions using the assimilative mapping of ionospheric electrodynamics technique, *J. Geophys. Res.*, *103*(A3), 4023.

Roelof, E. C., and A. J. Skinner (2000), Extraction of ion distributions from magnetospheric ENA and EUV images, *Space Sci. Rev.*, *91*, 437.

Ruohoniemi, J. M., and R. A. Greenwald (1998), The response of high-latitude convection to a sudden southward IMF turning, *Geophys. Res. Lett.*, *25*, 2913.

Sandel, B. R., et al. (2000), The Extreme Ultraviolet Imager investigation for the IMAGE mission, *Space Sci. Rev.*, *91*, 197.

Sandel, B. R., R. A. King, W. T. Forrester, D. L. Gallagher, A. L. Broadfoot, and C. C. Curtis (2001), Initial results from the IMAGE extreme ultraviolet imager, *Geophys. Res. Lett.*, *28*, 1439.

Smith, C. W., J. L'Heureux, N. F. Ness, M. H. Acuna, L. F. Burlaga, and J. Scheifele (1998), The ACE magnetic fields experiment, *Space Sci. Rev.*, *86*, 613.

Spasojević, M., J. Goldstein, D. L. Carpenter, U. S. Inan, B. R. Sandel, M. B. Moldwin, and B. W. Reinisch (2003), Global response of the plasmasphere to a geomagnetic disturbance, *J. Geophys. Res.*, *108*(A9), 1340, doi:10.1029/2003JA009987.

Williams, D. J., E. C. Roelof, and D. G. Mitchell (1992), Global magnetospheric imaging, *Rev. Geophys.*, *30*, 183.

Yoshikawa, I., M. Nakamura, M. Hirahara, Y. Takizawa, K. Yamashita, H. Kunieda, T. Yamazaki, K. Misaki, and A. Yamaguchi (1997), Observation of He II emission from the plasmasphere by a newly developed EUV telescope on board sounding rocket S-520-19, *J. Geophys. Res.*, *102*(A9), 19,897.

Yoshikawa, I., A. Yamazaki, K. Shiomi, M. Nakamura, K. Yamashita, and Y. Takizawa (2000a), Evolution of the outer plasmasphere during low geomagnetic activity observed by the EUV scanner onboard Planet-B, *J. Geophys. Res.*, *105*(A12), 27,777.

Yoshikawa, I., A. Yamazaki, K. Shiomi, K. Yamashita, Y. Takizawa, and M. Nakamura (2000b), Photometric measurement of cold helium ions in the magnetotail by an EUV scanner onboard Planet-B: Evidence of the existence of cold plasmas in the near-Earth plasma sheet, *Geophys. Res. Lett.*, *27*(21), 3657.

Yoshikawa, I., A. Yamazaki, K. Shiomi, K. Yamashita, Y. Takizawa, and M. Nakamura (2001), Interpretation of the He II (304 Å) EUV image of the inner magnetosphere by using empirical models, *J. Geophys. Res.*, *106*(A11), 25,745.

M. Hirai, G. Murakami, and I. Yoshikawa, Department of Earth and Planetary Science, Graduate School of Science, The University of Tokyo, 7-3-1 Hongo, Bunkyo, Tokyo 113-0033, Japan. (go@eps.s.u-tokyo.ac.jp)